J. Fluid Mech. (1996), *vol.* 309, *pp.* 301–319

On generation and convergence of polygonal-shaped shock waves

By N. APAZIDIS AND M. B. LESSER

Department of Mechanics, Royal Institute of Technology, 100 44 Stockholm, Sweden

(Received 18 August 1995 and in revised form 27 October 1995)

A process of generation and convergence of shock waves of arbitrary form and strength in a confined chamber is investigated theoretically. The chamber is a cylinder with a specifically chosen form of boundary. Numerical calculations of reflection and convergence of cylindrical shock waves in such a chamber filled with fluid are performed. The numerical scheme is similar to the numerical procedure introduced by Henshaw *et al.* (1986) and is based on a modified form of Whitham's theory of geometrical shock dynamics (1957, 1959). The technique used in Whitham (1968) for treating a shock advancing into a uniform flow is modified to account for non-uniform conditions ahead of the advancing wave front. A new result, that shocks of arbitrary polygonal shapes may be generated by reflection of cylindrical shocks off a suitably chosen reflecting boundary, is shown. A study is performed showing the evolution of the shock front's shape and Mach number distribution. Comparisons are made with a theory which does not account for the non-uniform conditions in front of the shock. The calculations provide details of both the reflection process and the shock focusing.

1. Introduction

Shock focusing remains an enduring problem. The reasons for this can be found in the phenomenon's continuing ability to provide surprising results. This acts as a touchstone for a number of interesting theoretical and experimental issues. The technical applications of shock waves further motivate their study. These range from problems caused by erosion to the deliberate cutting of hard surfaces. Medical applications, such as the disintegration of kidney and bladder stones, are rapidly expanding.

Experimental investigations of the behaviour of focusing wave fronts for a wide range of geometries and shock strengths have been presented by Sturtevant & Kulkarny (1976). Useful theoretical results concerning the nonlinear properties of the focusing process can be found in Cramer & Seebass (1978) and Cramer (1981). Recent papers by Henshaw, Smyth & Schwendemann (1986) and Schwendeman & Whitham (1987), using Whitham's theory of geometrical shock dynamics (1957, 1959), have been applied to the propagation of shocks of arbitrary strength into uniform media. Several key problems in the area of shock wave propagation have been analysed by means of a numerical procedure introduced in Henshaw *et al.* (1986). The procedure is based on the idea of shock wave tracking along rays perpendicular to the shock front's position. Propagation of shock waves in curved channels and diffraction of shocks by wedges and cylinders is investigated in Henshaw *et al.* The convergence

of polygonal-shaped, closed shock fronts is discussed by Schwendeman & Whitham (1987).

Recently cavitation, induced by the passage of shock waves in a liquid, has been a subject of experimental, numerical and theoretical work. Studies in which the passage of a plane shock over a cavity have been carried out by Dear, Field & Walton (1988) and Lesser & Finnström (1987). A more complex situation is examined by Gustafsson (1987). Here the shock wave propagates in a confined thin cylinder with an elliptic cross-section. A cylindrical shock wave is generated at one of the focal points of the chamber. The shock then reflects off the chamber wall and converges at the second focus. Linear theory was used in the calculations. Gustafsson found that the pressure distribution on the converging cylindrical wave front was non-homogeneous. The shock strength was shown to depend on the angle around the focus. *This occurs even though the pressure carried by the initial wave is uniform.* Gustafsson's device consisted of a fluid-filled elliptic chamber. The shocks were created by an electric discharge at one focus of the ellipse and converged at the other focus. This provided a convenient source of convergent cylindrical shocks. This type of device can be used in combination with a gel technique. The latter, which was developed for liquid impact studies, consists of the casting of a layer of gelatin from which any chosen shape may be cut and placed at a desired position (Dear & Field 1987). Therefore we suggest that this combination of techniques may serve for an experimental study of shock-induced cavity collapse, where the cavity shapes may be tailored to specific needs. A possible major drawback of such a device appears to be that the reflected cylindrical wave converges at the other focus with a pre-defined pressure distribution. In an experimental device, such as the one described above, it is desirable to control and vary the pressure distribution around the cavity.

The idea of influencing the pressure distribution on the reflected shock front by means of the chamber geometry has been developed by Apazidis (1992, 1993, 1994). This series of papers investigate shock propagation in cylindrical chambers both with elliptic and parabolic cross-sections. In addition the latter paper examines three-dimensional ellipsoidal and paraboloidal chambers. A major difference from Gustafsson's work is that the height of the chambers in the case of a two-dimensional configuration was not constant but varied slowly over the chamber domain. Thus a perturbed form of the two-dimensional calculation was carried out. It was shown that it is possible to tailor the flow and the pressure distribution behind the converging shock by changing the form of the chamber. A relation between the equation defining the upper surface of the chamber and the pressure distribution on the converging wave front was obtained. These calculations form a basis for the design of a shock generating device in which the strength distribution over the converging shock may be controlled. Such a device allows the experimental study of the influence of various types of pressure distributions on the collapse process. The main results of Apazadis' series of articles show that it is possible to create a cylindrical or plane shock wave with a predetermined pressure distribution by appropriate choice of the geometrical form of the reflector. The problem of shock reflection and propagation in these types of chambers has been treated analytically within the realm of the *linear* theory of sound pulses as described by Friedlander (1958). While this means that the results apply to weak shocks, they are of considerable use as guidance for our understanding the nonlinear case. The form of the reflector boundary was either elliptic or parabolic in two-dimensional configurations or ellipsoidal or paraboloidal in three-dimensional configurations. Therefore the reflected shock fronts were confined to cylindrical, spherical or plane shapes.

In the present work we consider other types of reflector boundaries. These types of reflectors will produce shock waves of arbitrary form and thus introduce a new degree of freedom in the shock generation process. The present analysis is not restricted to weak shocks but deals with shocks of arbitrary strength. The calculations are performed by means of a numerical procedure. This procedure is a modified form of the one introduced in Henshaw *et al.* (1986) based on geometrical shock dynamics. The modifications involve two aspects of the calculations. Straightforward minor changes, which like previous works make extensive use of spline techniques, have some interest in their own right. This is required for the treatment of reflections which require some new procedures. The second modification is of greater importance and involves the treatment of a non-uniform flow in advance of the shock. This is necessary as we are treating shocks of arbitrary strength which are created by a reflection process. Thus the reflected shock is propagating into the disturbance created by the incident wave. The technique used for this is based on the invariance properties of the problem to Galilean transformations, as pointed out in Whitham (1968). Extra terms are introduced into the equations of motion due to the non-uniformity of the flow. Comparisons are made with calculations that ignore the flow non-uniformity or even the flow itself ahead of the shock. The results of the calculations show that it may be possible to create shock waves of arbitrary form. Of special interest are polygonal-shaped shocks with plane sides and sharp corners. Such shocks have been considered in a number of the above references. In the present paper particular attention is given to the possible experimental creation of such shocks. The convergence and evolution properties discussed by previous workers are also confirmed and extended.

2. Formulation

The main objective of the present work is to examine the possibility of the generation of two-dimensional polygonal-shaped shock waves by a process of reflection from a smooth boundary. The sharp corners will arise as a feature of the shock reflection and focusing. For this purpose consider a confined two-dimensional chamber filled with fluid. The process is initiated by the creation of a cylindrical shock wave with constant Mach number distribution along the shock front. This is generated at the centre of the chamber. This could be done by a controlled explosion or electric discharge as in the work of Gustafsson (1987). A convenient representation of the chamber boundary is given in parametric form by the equation

$$r = \frac{1}{1 + \varepsilon \cos(n\phi)}. \tag{1}$$

This can be interpreted as representing a perturbation of a circle by a cosine function multiplied by a small parameter ε. The resulting shapes of the reflector boundary for $n = 4$ and 5 are shown in figure 1. The motivation for this choice is that it is well known that a circular wave front will reflect as a plane wave off a parabolic boundary. While this is not a parabolic boundary, the regions around the maxima and minima quadratically approximate one. Therefore, dependent on the periodicity of the perturbation, it is expected that such a reflecting surface will produce a form that will tend to planarity about these points. It will be seen that this planarity is further emphasized by the shock convergence. This follows the work of Whitham, where the tendency to planarity of shocks is explicitly calculated.

Three different stages of shock propagation in the chamber are identified. The first stage is the propagation of the initial outgoing cylindrical shock. This stage starts

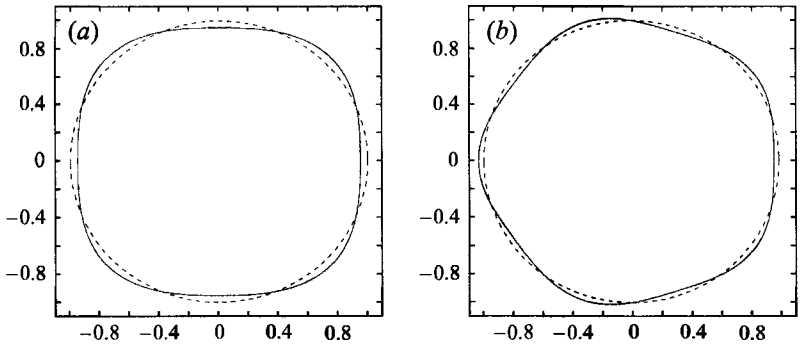

FIGURE 1. Reflector boundaries for (*a*) $n = 4, \varepsilon = 0.05$ and (*b*) $n = 5, \varepsilon = 0.035$. The corresponding circles are shown by dashed lines.

with the formation of the shock at the centre of the chamber. The shock is assumed to have uniform strength along its front. The strength will vary with the propagating shocks position. This stage is completed when the first points of the outgoing wave come into contact with the reflector boundary. This initiates the second stage, which is the reflection itself as described in § 3. The end of the reflection stage is reached when a connected reflected wave front is formed, i.e. the reflection process has terminated. The last stage of this process is the convergence of the fully formed reflected wave. The convergence of the wave is investigated in § 4.

This assumption of uniform strength provides a standard solution of the initial stage and therefore any particular shock strength may be chosen for the commencement of the reflection stage. In the numerical calculations the shock strength at this point is taken as $M = 2$, which provides the necessary initial data. In some of the calculations a 'blast-wave' similarity solution is employed. The energy is normalized so as to fulfil the above Mach number condition at reflection. It is important to realize that the shock strength distribution will be changing during the reflection phase. The value of $M = 2$ only applies at the initial points of contact of the incident shock with the boundary. Oblique shock relations are used to calculate the local reflection properties. Therefore the calculation is fully nonlinear. Because the angle of incidence is extremely oblique there are no evident problems with Mach reflection effects.

Our calculations use geometrical shock dynamics or GSD developed by Whitham. This theory extends the ideas of geometrical optics or wave propagation. The main idea is that the speed of propagation along the ray depends on the value of the Mach number at the considered location. The value of the local Mach number M is in turn coupled to the ray-tube area A by means of a relation between the area of a ray tube and the shock Mach number, called the A–M relation and given by

$$A = A_0 \frac{f(M)}{f(M_0)}, \tag{2}$$

where M_0 and A_0 are the initial values of the Mach number and ray-tube area respectively. From a differential geometric point of view the relation represents the Jacobian of the transformation of the shock front as it propagates. Function $f(M)$ in the A–M relation was obtained by Whitham (1957) by writing the conservation equations of motion in characteristic form and applying the shock relations along the characteristic in the direction of propagation. This ad-hoc approach provided a closed set of equations leading to the above relation. In addition to a number of heuristic arguments justifying such a scheme there is now a considerable body of evidence

indicating that it leads to excellent results in a number of cases. Some exceptions have been noted by Prasad (1992), who claims to have developed a form of GSD as a first stage of a rational approximation technique for shock propagation problems. It is also claimed in Prasad's work that in some cases GSD may lead to erroneous results. The ultimate resolution of this matter must rest on experimental evidence, and the present calculations combined with future experiments may be of some help in this matter. Following Whitham's approach the function $f(M)$ takes the form

$$f(M) = \exp\left(-\int \frac{M\lambda(M)}{M^2-1}\mathrm{d}M\right), \tag{3}$$

where

$$\lambda(M) = \left(1 + \frac{2}{\gamma+1}\frac{1-\mu^2}{\mu}\right)\left(1 + 2\mu + \frac{1}{M^2}\right), \tag{4}$$

$$\mu^2 = \frac{(\gamma-1)M^2+2}{2\gamma M^2-(\gamma-1)}, \tag{5}$$

and where γ is the ratio of specific heats (= 1.4 for air). A similar relation follows for liquids. Water is a particular example where γ may be taken as approximately 7 and is interpreted as the exponent in the Tait equation for the pressure density equation of water.

The equations of geometrical shock dynamics, by means of which the shock front positions $r(x, y)$ are calculated, may be put in the following form, see Whitham (1974), Henshaw *et al.* (1986):

$$\frac{\mathrm{d}}{\mathrm{d}t}\boldsymbol{r}(t) = M(t)\boldsymbol{n}(t), \tag{6}$$

where $\boldsymbol{n}$ is the normal to the shock front. This system of nonlinear differential equations together with the A–M relation provides a complete set of equations for evaluation of the shock front position and strength as a function of time. These equations are treated following a procedure based on that of Henshaw *et al.* (1986).

2.1. *Propagation into a non-uniform region*

The above equations, used by previous investigators, are derived under the assumption of quiescent conditions ahead of the advancing shock. Clearly this is not the case under the conditions of reflection. It can be argued that the flow field created by the incident shock rapidly decreases in amplitude and that one only has to make an additive or linear correction to the result. This is implicit in the work of Gustafsson (1987). A modification of GSD was carried out by Whitham (1968) to account for uniform conditions ahead of the shock. In this elegant approach Whitham used Galilean invariance to transform the basic GSD equations to a reference frame which was at rest with respect to the oncoming flow. Among other corrections, this showed that the ray tubes would not be orthogonal to the shock surfaces. In the following we follow this idea to develop equations for the case of non-uniform conditions. The basis for this is that the shock is merely a surface of discontinuity and possesses no mass, therefore it is possible to use a 'local' Galilean transformation to derive suitable equations of motion from the formulation in a frame with no flow ahead of the shock. Because of the gradient in flow conditions new terms appear in the relevant equations.

To generalize Whitham's formulation to a non-homogeneous flow field ahead of the shock consider two coordinate frames F and F'. Let F be a fixed frame described

by (x, y, t) and F' a moving frame in which the medium ahead of the shock is *locally* at rest. Transformation between the two frames is given by

$$x = x' + U(x, y)t', \quad y = y' + V(x, y)t', \quad t = t'. \tag{7}$$

In frame F' the shock position at time t' is given by

$$a_0 t' = \alpha'(x', y'), \tag{8}$$

where a_0 is the sound speed. The shock velocity is perpendicular to the shock front and its magnitude is given by $a_0 M'$, where M' is the shock Mach number in the moving frame

$$M' = \left(\alpha_{x'}'^2 + \alpha_{y'}'^2\right)^{-1/2}. \tag{9}$$

In the fixed frame F we have a similar relation describing the shock front position

$$a_0 t = \alpha(x, y). \tag{10}$$

Following Whitham's approach, we relate the two descriptions by means of the coordinate transformation and obtain

$$a_0 t = \alpha'(x - U(x, y)t, y - V(x, y)t), \tag{11}$$

and thus

$$\alpha = \alpha'(x - u(x, y)\alpha(x, y), y - v(x, y)\alpha(x, y)), \tag{12}$$

where $u = U/a_0$ and $v = V/a_0$. In the moving frame F' the medium ahead of the shock is at rest and the equations of GSD apply. Thus the function $\alpha'(x', y')$ satisfies the equation

$$\frac{\partial}{\partial x'}\left(\frac{M'}{A'}\frac{\partial \alpha'}{\partial x'}\right) + \frac{\partial}{\partial y'}\left(\frac{M'}{A'}\frac{\partial \alpha'}{\partial y'}\right) = 0, \tag{13}$$

where

$$M' = \left(\alpha_{x'}'^2 + \alpha_{y'}'^2\right)^{-1/2}. \tag{14}$$

and

$$A' = f(M'). \tag{15}$$

We now use (12) and find the relations between the partial derivatives in the two coordinate frames. We have

$$\left.\begin{aligned} \frac{\partial}{\partial x} &= (1 - u_x\alpha - u\alpha_x)\frac{\partial}{\partial x'} + (-v_x\alpha - v\alpha_x)\frac{\partial}{\partial y'}, \\ \frac{\partial}{\partial y} &= (-u_y\alpha - u\alpha_y)\frac{\partial}{\partial x'} + (1 - v_y\alpha - v\alpha_y)\frac{\partial}{\partial y'}. \end{aligned}\right\} \tag{16}$$

Solving for the $\partial/\partial x'$ and $\partial/\partial y'$ we obtain

$$\left.\begin{aligned} \frac{\partial}{\partial x'} &= \frac{(1 - v_y\alpha - v\alpha_y)\dfrac{\partial}{\partial x} + (v_x\alpha + v\alpha_x)\dfrac{\partial}{\partial y}}{(1 - v_y\alpha - v\alpha_y)(1 - u_x\alpha - u\alpha_x) - (v_x\alpha + v\alpha_x)(u_y\alpha + u\alpha_y)} \\ \frac{\partial}{\partial y'} &= \frac{(u_y\alpha + u\alpha_y)\dfrac{\partial}{\partial x} + (1 - u_x\alpha + u\alpha_x)\dfrac{\partial}{\partial y}}{(1 - v_y\alpha - v\alpha_y)(1 - u_x\alpha - u\alpha_x) - (v_x\alpha + v\alpha_x)(u_y\alpha + u\alpha_y)} \end{aligned}\right\} \tag{17}$$

Applying the latter to α' we find

$$\left.\begin{aligned}\alpha'_{x'} &= \frac{\alpha_x + \alpha(\alpha_y v_x - \alpha_x v_y)}{\Delta} \\ \alpha'_{y'} &= \frac{\alpha_y + \alpha(\alpha_x u_y - \alpha_y u_x)}{\Delta}\end{aligned}\right\} \tag{18}$$

where Δ is the determinant of (16) or denominator in (17).

Equation (13) for α' in the moving frame is thus transformed to the following form in the fixed frame:

$$\begin{aligned}&(1 - v_y\alpha - v\alpha_y)\frac{\partial}{\partial x}\left(\frac{M'}{A'}\frac{\alpha_x + \alpha(\alpha_y v_x - \alpha_x v_y)}{\Delta}\right) \\ &+(v_x\alpha + v\alpha_x)\frac{\partial}{\partial y}\left(\frac{M'}{A'}\frac{\alpha_x + \alpha(\alpha_y v_x - \alpha_x v_y)}{\Delta}\right) \\ &+(u_y\alpha + u\alpha_y)\frac{\partial}{\partial x}\left(\frac{M'}{A'}\frac{\alpha_y + \alpha(\alpha_x u_y - \alpha_y u_x)}{\Delta}\right) \\ &+(1 - u_x\alpha - u\alpha_x)\frac{\partial}{\partial y}\left(\frac{M'}{A'}\frac{\alpha_y + \alpha(\alpha_x u_y - \alpha_y u_x)}{\Delta}\right) = 0.\end{aligned} \tag{19}$$

The idea is now to transform (19) to the divergence form. It becomes

$$\nabla \cdot (\boldsymbol{e}/A) = 0, \tag{20}$$

where $\boldsymbol{e}$ is the unit vector along the ray direction. Note that as discussed $\boldsymbol{e}$ is in general *not* normal to the shock front. This formality of stating (19) in divergence form is needed to develop the expressions for the ray unit vector $\boldsymbol{e}$, area A' and Mach number M' in the moving frame. We thus obtain

$$\boldsymbol{e} = \frac{(E_x, E_y)}{(E_x^2 + E_y^2)^{1/2}}, \tag{21}$$

where

$$E_x = (1 - \alpha v_y - \alpha_y v)\left[\alpha_x + \alpha(\alpha_y v_x - \alpha_x v_y)\right] + (\alpha u_y + \alpha_y u)\left[\alpha_y + \alpha(\alpha_x u_y - \alpha_y u_x)\right], \tag{22}$$

and

$$E_y = (1 - \alpha u_x - \alpha_x u)\left[\alpha_y + \alpha(\alpha_x u_y - \alpha_y u_x)\right] + (\alpha v_x + \alpha_x v)\left[\alpha_x + \alpha(\alpha_y v_x - \alpha_x v_y)\right]. \tag{23}$$

The area A' and the Mach number M' in the moving frame are also expressed in terms of α, u and v and their derivatives:

$$M' = \frac{(1 - \alpha v_y - \alpha_y v)(1 - \alpha u_x - \alpha_x u) - (\alpha v_x + \alpha_x v)(\alpha u_y + \alpha_y u)}{\left(\left[\alpha_x + \alpha(\alpha_y v_x - \alpha_x v_y)\right]^2 + \left[\alpha_y + \alpha(\alpha_x u_y - \alpha_y u_x)\right]^2\right)^{1/2}} \tag{24}$$

and

$$A = A'(\boldsymbol{e} \cdot \boldsymbol{n}). \tag{25}$$

Thus, as shown earlier by Whitham (1968) A' is the area cut out by the ray tube and A is the normal cross-section.

The flow field ahead of the converging shock is the one that is produced by the initial outgoing cylindrical shock. It is convenient to have as explicit a solution as possible for the associated flow field. Therefore the well-known blast wave solution of

a spherical explosion obtained numerically by Taylor (1950) and analytically by Sedov (1946) will be utilized here to describe the flow field ahead of the converging shock. Using Sedov's solution for the cylindrical blast wave, described in detail in Hayes & Probstein (1966, pp. 56–70), we obtain an expression for the radial component $w(r)$ of the velocity field behind the shock at each location in the chamber. The Cartesian components of the velocity field u and v and their derivatives are then calculated in a standard manner as

$$u = w\cos\theta, \qquad v = w\sin\theta, \tag{26}$$

$$u_x = w_r\cos^2\theta + w/r\sin^2\theta,\ u_y = (w_r - w/r)\sin\theta\cos\theta, \tag{27}$$

$$v_x = (w_r - w/r)\sin\theta\cos\theta,\ v_y = w_r\sin^2\theta + w/r\cos^2\theta. \tag{28}$$

It should be noted that the blast wave solution is used for convenience and is not an intrinsic necessity. It only strictly applies to very strong initial shocks with zero counter-pressure. However because the flow rapidly decays behind the initial front it is felt to be reasonably useful for our purposes.

3. Reflection

The creation of a polygonal-shaped shock is initiated by reflecting a cylindrical wave from a perturbed circular boundary. This is represented by the parametric form given by equation (1).

The process starts with an outgoing cylindrical wave with a Mach number distribution which is a function only of its radius. The shock Mach number of the outgoing wave just before the first contact with the reflector boundary is M_i. As only the initial contact points of the wave will have this Mach number, it is necessary to calculate the change in Mach number undergone by successive segments as they travel the distance from the initial position to the contact. We then calculate the Mach number M_b at each point of the wave front just before contact with the reflector boundary. This could be done using exact relations in certain special cases. In general it is necessary to use an approximate approach such as a calculation done by means of the A–M relation with GSD, i.e.

$$\frac{A_i}{A_b} = \frac{f(M_i)}{f(M_b)}. \tag{29}$$

Here A_i is the initial ray-tube area and A_b is the ray-tube area of the outgoing cylindrical wave just before the contact with the reflector boundary. The appropriate incident Mach number, i.e. M_b, and the ray-tube area of the wave at the reflector boundary A_b preceding the reflection are used to calculate the Mach number of the reflected wave. To perform this we make a coordinate transformation and consider the reflection process from the point of view of an observer moving with the point of intersection C between the incident shock and the reflector boundary, see figure 2. By means of such a transformation the incident and reflected shocks are viewed from a reference frame in which they are stationary. The flow field, as seen by such an observer, is shown in figure 2 and represents a regular reflection of a stationary oblique shock. It is well known that in such a case the reflected shock wave is not specularly reflected, that is the angle β_3 between the reflected wave and the boundary is not equal to β_1, the corresponding angle between the incident shock and the boundary. Standard relations provide the angle β_3 and also the reflected wave Mach number M_r just after the reflection, from β_1 and M_b. For a detailed discussion see e.g. Anderson (1990).

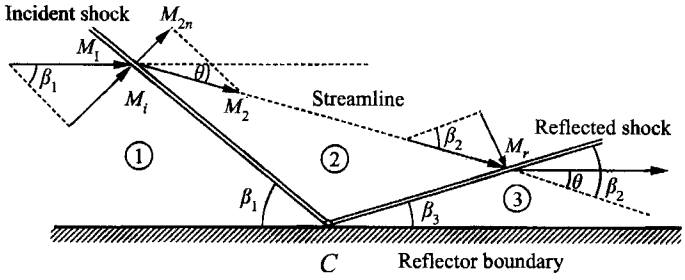

FIGURE 2. Reflection of an incoming oblique shock from the boundary.

These relations show that the flow field local to the point of contact is separated into three regions: region 1 ahead of the incident shock; region 2 behind the incident, or ahead of the reflected shock; and finally region 3 behind the reflected shock. This is shown in figure 2. The normal component of the Mach number M_{2n} behind the incident shock is given by the Mach number relation across the incident shock

$$M_{2n} = \left[\frac{M_i^2 + 2/(\gamma - 1)}{2\gamma/(\gamma - 1)M_i^2 - 1}\right]^{1/2}. \tag{30}$$

The deflection angle θ is found by the usual θ–β–M relation,

$$\tan\theta = \frac{(M_i^2 - 1)\sin 2\beta_1}{M_i^2(\gamma + \cos 2\beta_1) + 2\sin^2\beta_1}, \tag{31}$$

formulated here in terms of the normal component of the incident Mach number. The Mach number M_2 behind the incident shock is then

$$M_2 = \frac{M_{2n}}{\sin(\beta_1 - \theta)}, \tag{32}$$

and the θ–β–M relation may again be used, in this case to obtain the shock wave angle β_2,

$$\frac{2}{\tan\beta_2}\left[\frac{M_2^2\sin^2\beta_2 - 1}{M_2^2(\gamma + \cos 2\beta_2) + 2}\right] = \tan\theta. \tag{33}$$

The reflection angle β_r and the Mach number of the reflected wave front M_r at the moving point of contact are then easily obtained from the geometric relations

$$\beta_r = \beta_3 = \beta_2 - \theta, \tag{34}$$

and

$$M_r = M_2 \sin\beta_2. \tag{35}$$

The above provides an algorithm for calculating the reflected shock parameters as the incident wave sweeps the boundary. This process terminates with a closed reflected shock, and no remaining incident front. Thus the Mach number M_r of the reflected wave at each point of the reflector boundary just after the reflection, as well as the normal to the reflected wave front $\boldsymbol{n}_r$ are now known quantities. The numerical procedure for calculating the propagation of the reflected shock uses many of the ideas in the scheme described by Henshaw *et al.* (1986). The main difference is that, as discussed above, account is taken of the non-uniform flow produced by the incident wave field which is ahead of the reflected shock. Some additional small modifications are intended for dealing with the shock front reflection itself. The

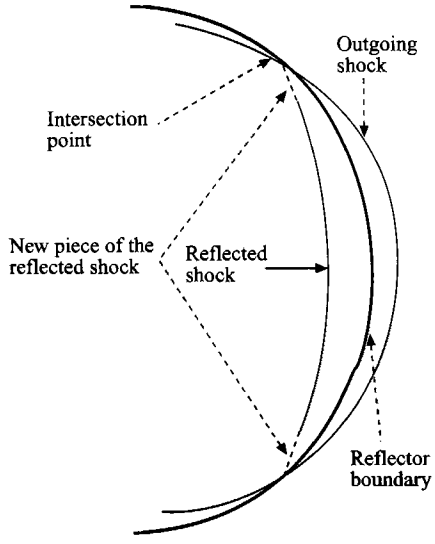

FIGURE 3. Propagation and construction of the reflected wave.

previous work only involved diffraction rather than reflection effects. The ideas of shock wave tracking along the approximate rays, and representing the shock front position $r_j(t)$, $j = 1, ..., N$ by a discrete set of points at each time t follows Henshaw *et al.* The differential equation for the shock front position is written in the usual ray trajectory form

$$\frac{\mathrm{d}}{\mathrm{d}t} r_j(t) = M_j(t) e_j(t), \quad j = 1, ..., N, \tag{36}$$

where $e_j(t)$ is the unit vector along the ray that describes the shock path when it is moving into a non-uniform region. Note that in order to calculate e it is necessary to have expressions for the oncoming flow field and suitable gradients of this field. In the present paper this, as previously noted, is accomplished by using the blast wave solution for a cylindrically symmetric explosion to calculate both e and M', the Mach number relative to the oncoming flow. Expressions for the components of e were given in the previous section. It is important to realize that the $A(M)$ relation applies in the local frame fixed to the oncoming flow, i.e. to a frame in which the shock is propagating into a region that is locally at rest. To emphasize this one could distinguish the Mach number in the local rest frame and the area – Mach number relation, for example by denoting it as M' and the function $A'(M')$. For the purposes of this presentation this formality is not needed, but of course it is accounted for in the actual numerical calculations. It is also worth stating that the shock is not normal to the ray direction e.

As noted above the reflected wave front is constructed by finding the points where the outgoing wave first comes into contact with the reflector boundary see figure 3. Using the symmetry of the problem the development of the reflected wave is followed starting at *one* of these points.

A new differential segment of the reflected wave is added as a line between the endpoint of the reflected wave front and the reflector boundary. The inclination of this added line segment is defined by the direction perpendicular to e_r, i.e. the direction of the ray to the calculated reflected wave front at the endpoint. It is desirable to maintain as uniform a distribution of defining points along the developing wave as

convenient. To this end the decision as to addition of a new segment of reflected wave is based on the existing point distribution. At each time step the distance between defining points, that is points on the developing rays, will change. This procedure of point distribution is different than that used by Henshaw *et al.* where no reflections were calculated.

The Mach number distribution on the added line segment is the one calculated in accordance with consideration of the reflection relations and the appropriate transformation to a frame locally at rest with respect to the oncoming flow. This new wave front expanded by a small line segment is advanced along the ray direction with velocity proportional to the Mach number obtained by means of the A–M relation (with due respect to the appropriate frame transformation as noted above)

$$\frac{A_j(t)}{A_j(0)} = \frac{f(M_j(t))}{f(M_j(0))}, \tag{37}$$

where $A_j(0)$ and $M_j(0)$ indicate the initial area and Mach number distribution. This procedure was necessary to provide the accuracy needed for a proper treatment of the oblique reflection process.

An explicit second-order Runge–Kutta time-marching scheme is used to propagate the shock along a ray. The number of points N along the wave front is kept constant. This means that each time when a small line segment is added to the wave front, in accordance with the procedure described above, a spline approximation to the discrete wave front is calculated and the points on the shock front are linearly redistributed. The same procedure is applied to the Mach number distribution along the shock front. This new wave front with the corresponding Mach number distribution is then chosen as the initial one. Also a smoothing procedure described in Henshaw *et al.* (1986) is applied to the wave front at every n_s time steps (usually 20), thus

$$\tfrac{1}{2}\left[\boldsymbol{r}_j(t) + \boldsymbol{r}_{j-1}(t)\right] \rightarrow \boldsymbol{r}_j(t). \tag{38}$$

The smoothed shock front with the corresponding Mach number distribution is then again chosen as the initial shock front and saved.

The results of the reflection calculations for $n = 4$ and $n = 5$ are shown in figures 4 and 5. Figure 4(*a*) shows the formation of the reflected shock on an exaggerated scale which emphasizes the local parabolic nature of the reflecting surface and the resulting tendency toward local planarity. It is also evident from this figure that the refined splining technique provides a smooth transition to the reflected shock geometry. Figure 4(*b*) shows an overview on a more representative scale which indicates the tendency toward a polygonal form for the reflected wave. Finally figure 4(*c*) displays the relationship between the position of the reflected wave and the Mach number of the wave. The reader should observe that the actual scale of the Mach number variations is quite small and is exaggerated in the figures. Figure 5 presents the same type of information for the case of a boundary with pentagonal symmetry. The Mach number gradient indicates the formation of shock-shocks, therefore we see that the solution can be thought of as a periodic array of shock-shocks which rotate about the wave front. This will become evident when we observe families of shock front plots.

4. Focusing

We now possess the initial data needed to follow the development of the shock front as it converges into the centre of the cylindrical region. For the most part

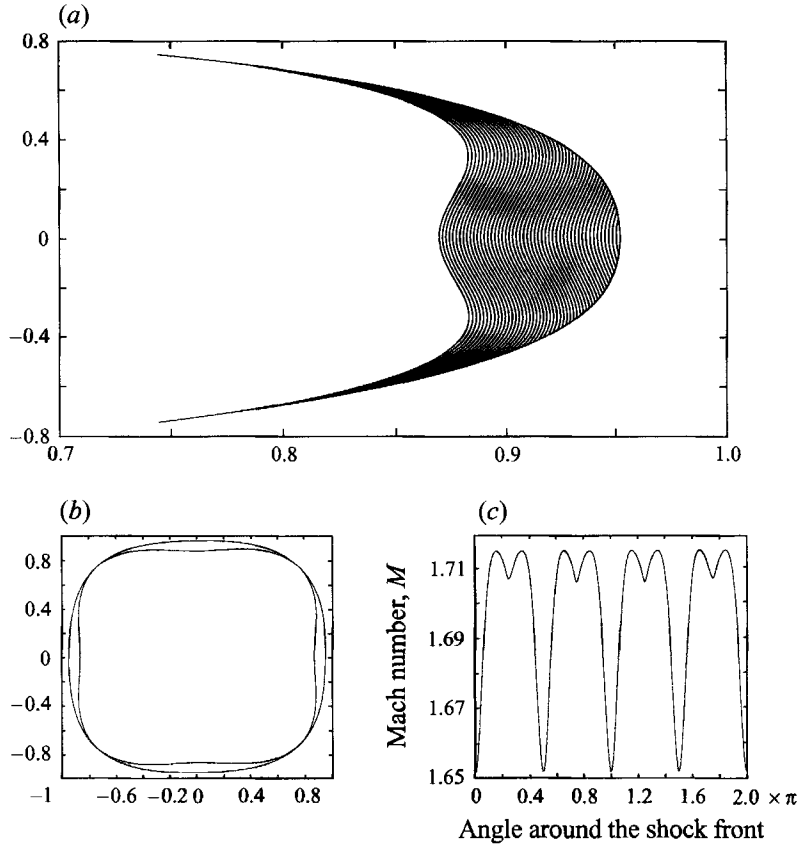

FIGURE 4. Reflected wave fronts for $n = 4$. (*a*) Reflected wave fronts in a sector of a reflector. (*b*) Fully reflected wave front within a reflector. (*c*) Mach number distribution on the fully reflected wave front.

we follow Henshaw's method. The main modification is the account taken of the oncoming flow as described in the previous section. Formally the change is in the use of the ray direction $\boldsymbol{e}$ rather than the shock normal $\boldsymbol{n}$. Also account must be taken of the modified $A(M)$ relation suitable to the local advancing frame in which the oncoming flow is at rest. Thus apply a two-step leap-frog scheme to equation (36),

$$\boldsymbol{r}_i(t + \Delta t) = \boldsymbol{r}_i(t - \Delta t) + 2\Delta t M_i(t)\boldsymbol{e}_i(t), \quad i = 1, ..., N. \tag{39}$$

With converging shocks the points on the shock front tend to cluster and spread out in compressive and expansive regions of the shock front. Following Henshaw we delete and insert points on the shock. The number of points along the shock front N now varies. To reduce the high-frequency oscillations the same smoothing procedure (38) as in the previous section is applied every n_s time steps (usually 20). It is desirable to calculate the spline approximation to the discrete points along the shock front and the Mach number distribution and then redistribute the points homogeneously along the front. The number of points chosen in such a redistribution N_s (usually 500) is constant. The spline approximations are calculated after the smoothing procedure is applied to the shock front. These smoothed shock fronts and Mach number distributions are then used as initial ones and are stored.

The Courant–Friedrichs–Lewy stability condition has to be checked and satisfied.

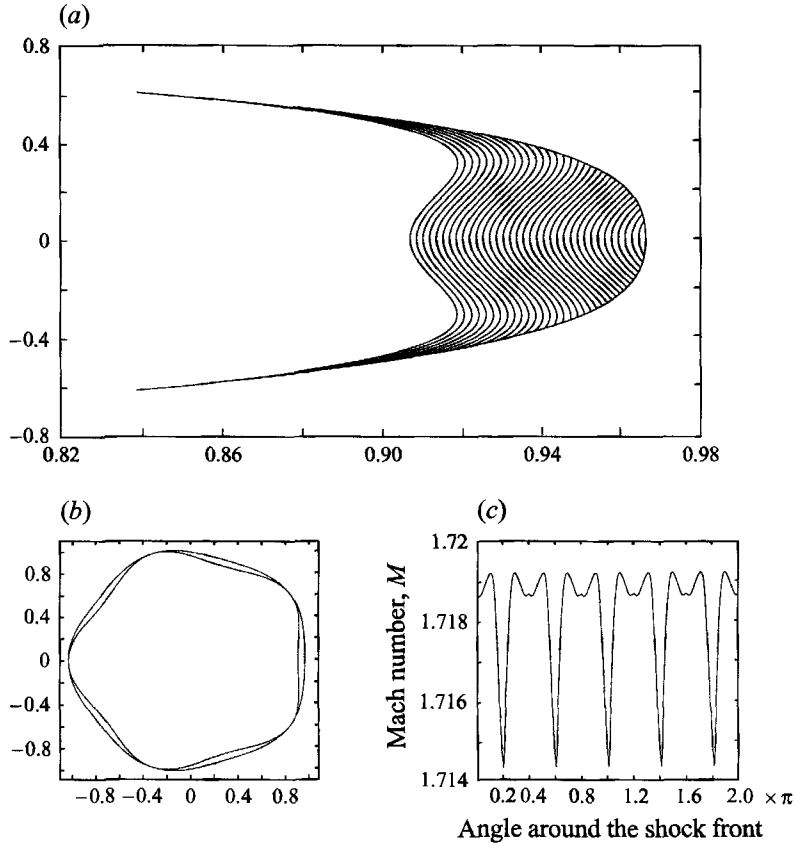

FIGURE 5. Reflected wave fronts for $n = 5$. (*a*) Reflected wave fronts in a sector of a reflector. (*b*) Fully reflected wave front within a reflector. (*c*) Mach number distribution on the fully reflected wave front.

As pointed out by Schwendeman & Whitham (1987) the average spacing between the points along the wave front will decrease for converging shocks. We therefore choose the time-step increment Δt so that the above mentioned stability condition is

$$\frac{\Delta t}{\Delta s_{min}} < K = O(1), \tag{40}$$

where usually $K = 0.15$ is satisfied at each integration step. Since the spacing between the points on the wave front Δs will decrease through the convergence process so will the time-step increment Δt. The periodicity condition for the converging shocks

$$r_1(t) = r_N(t), \tag{41}$$

used by Schwendeman & Whitham (1987) is also applied in the present calculations.

Shock front positions of the converging shocks, advancing into an inner region of the reflector with the flow field created by the outgoing cylindrical shock, are shown in figure 6. Four different types of reflector boundaries with $n = 4, 5, 6$ and 8 are plotted. It is clearly seen that initially smooth curved forms of the reflected waves tend to become planar, build corners with high curvature and eventually form polygonal-like shock fronts. When such shock fronts are formed they are reoriented to the reflector boundary, that is corners are formed opposite to the flat portions and plane sides

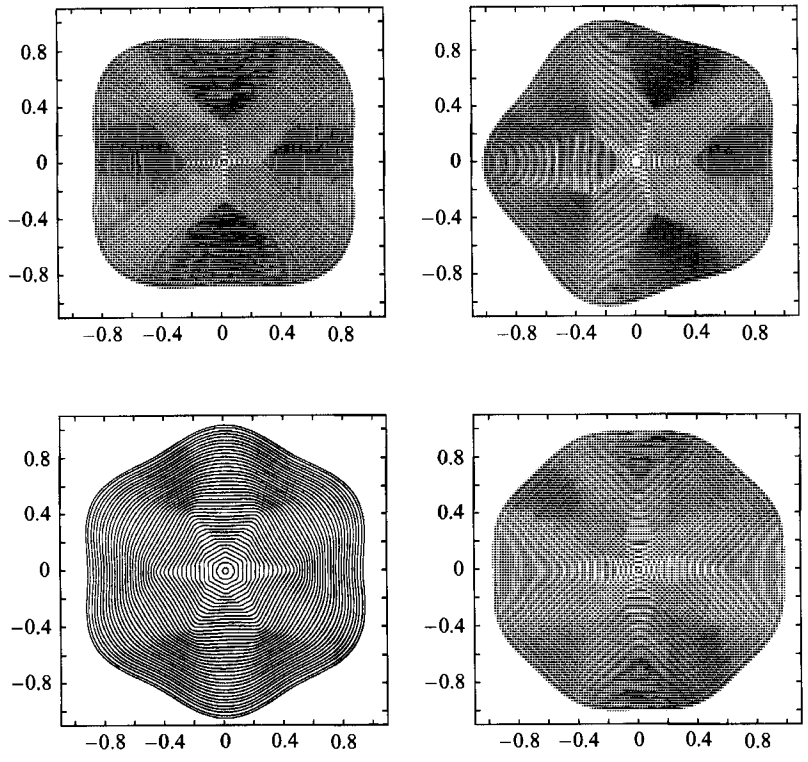

FIGURE 6. Successive positions for the converging shock fronts with initial Mach number $M = 2$, for $n = 4, 5, 6$ and 8.

opposite to the smooth corners of the reflector. All these properties of the converging shocks with the exception of the initial Mach number distribution, are quite similar to the case of pure polygonal shapes of the initial front, investigated in detail by Schwendeman & Whitham (1987). According to this study these polygonal-shaped shock fronts once they are formed, will be repeated and reoriented during the later stages of the convergence process. It is important to realize that the situation in this case is slightly different as instead of a pure polygonal boundary we have a boundary with high curvature at the 'corners'. The spline technique used in the calculations maintains the smoothness of the geometry. In the present work we are interested what will result in an actual experiment where the incoming geometry is produced by reflection off a perturbed boundary. Schwendeman & Whitham do treat a case in which the initial shock shape is perturbed from one with pure polygonal form and which results in convergence to a sharp corner. The shape seen in this calculation, which is into a region at rest, is quite similar to the cases seen here.

As a comparison calculations were done for higher values of the initial Mach number than $M = 2$ which was used for the case shown in figure 6. In figure 7 we compare the focusing process for the cases $n = 4$ and $n = 5$ with initial Mach numbers $M = 2$ (figure 7*a*, *c*) and $M = 5$ (figure 7*b*, *d*). It should be mentioned at this point that the difference in the values of the reflected Mach number between these two cases is not great, since the maximum value of the reflected Mach number for any value of the inital Mach number cannot exceed $M \approx 2.6$. The main difference in the pattern of the converging process here is due to the difference in the strength of

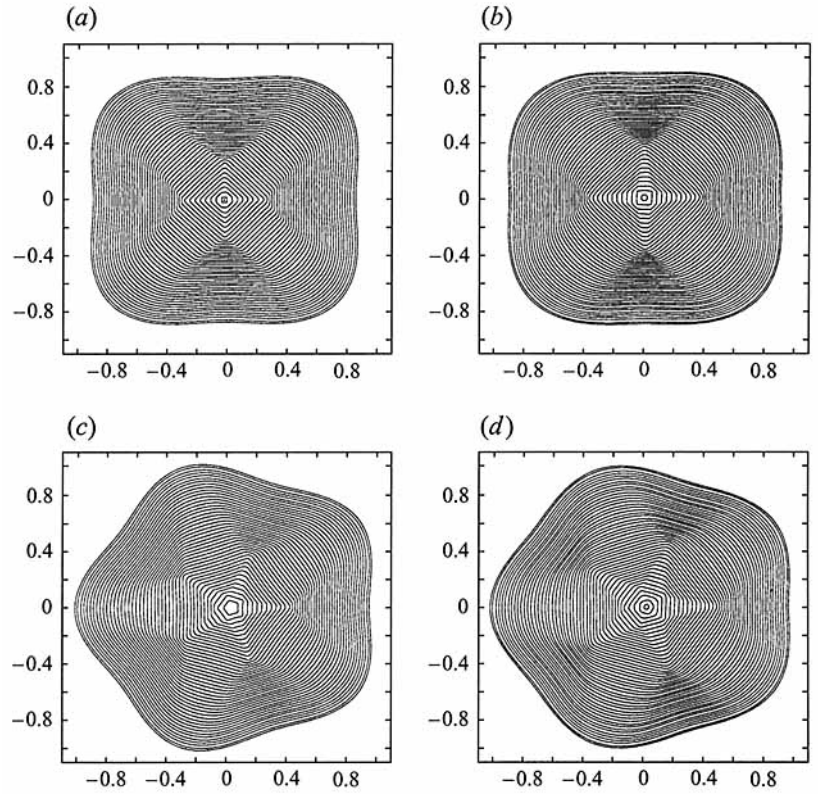

FIGURE 7. Converging shock waves for $n = 4$ and $n = 5$ with initial Mach numbers: (*a*,*c*) $M = 2$; (*b*,*d*) $M = 5$.

the flow ahead of the shock. A higher value of the Mach number of the flow ahead of the shock tends to enhance the effect of the shock transformation as seen here.

The reflector boundary together with two shock fronts and corresponding Mach number distributions for $n = 4$ are shown in figure 8. One of the shock fronts in each figure is chosen at the beginning of the convergence process and is thus in the vicinity of the reflector boundary, and the second one is chosen at a later time during the formation of a square shock front. Figures 8(*a*) and 8(*b*) show the shock fronts and corresponding Mach number distributions of the calculations with and without flow ahead of the converging shocks, respectively. This figure shows similarities and differences in the converging processes of shocks with and without flow ahead. The formation of a polygonal-shaped shock is of a similar nature in these two cases. Comparing the shock fronts at the chosen moments, in both cases one may still observe flat portions on the shock fronts that are parallel with the flatter portions of the reflector boundary. These will shortly disappear and a corner of a square shock opposite to the flatter side of the reflector will be formed. This may be explained by the Mach number distributions shown in the same figure. The value of the Mach number on the flat portions parallel to the reflector boundary is much less than on the increasing flat portions of the shock front corresponding to the corners of the reflector boundary. The portions of the shock front with lower Mach number values are travelling slower and are therefore absorbed by the faster parts of the shock.

The difference between the cases with and without flow ahead of the shock is also

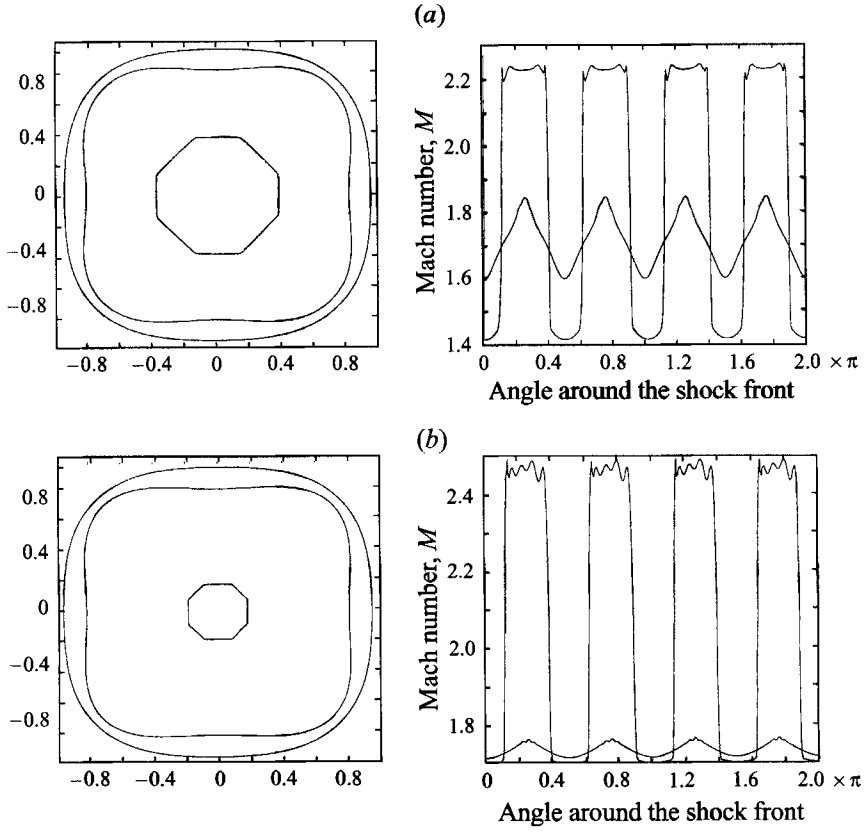

FIGURE 8. Two shock positions with corresponding Mach number distributions for $n = 4$. (*a*) Calculations with flow ahead of the shock and (*b*) with no flow ahead of the shock.

clearly seen here. We may see that a shock front comparable to the one in figure 8(*a*) is formed at a later instant and thus further into the reflector in the case of no flow ahead shown in figure 8(*b*). Also the Mach number distribution in figure 8(*a*) indicates the influence of the flow field ahead of the shock. Mach number is increased on the portions of the shock corresponding to the corners of the boundary and decreased on the portions corresponding to the flatter parts of the boundary. In the case of no flow ahead, figure 8(*b*), there is almost no decrease in the values of the Mach number. This is due to the fact that flow ahead of the shock is considerably reduced by the time the shock front has reached the position in the inner part of the chamber as shown in figure 8(*a*). The high-frequency fluctuations on the upper portions of the Mach number distribution seen in figure 8 are of a numerical nature and originate from the numerical solution of the nonlinear area–Mach number relation. Their influence on the form of the shock front is of minor importance as long as their relative value compared to the jump in the Mach number distribution is small.

5. Conclusions

The primary purpose of this work was to examine the feasibility of producing polygonal shocks by reflecting cylindrical waves off a perturbed circular boundary. It was known from the previous work of Whitham that shocks with corners can be stable in form. The proposed geometry introduces a complication that requires

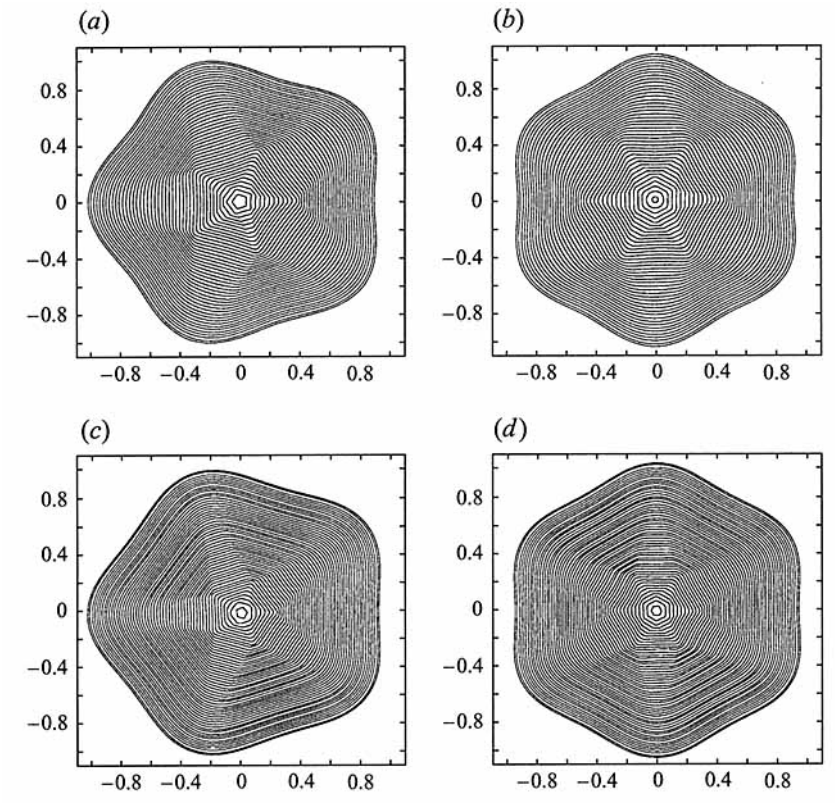

FIGURE 9. Successive shock positions for the converging shock fronts with initial Mach number $M = 2$: (a, b) with and (c, d) without flow ahead.

some minor modifications of GSD as formulated by Whitham due to the flow field created by the initial incident cylindrical shock. The point of departure was Whitham (1968) which generalized the GSD equations to account for a uniform flow ahead of the shock. In the present case the flow is not uniform and the technique of transforming to a frame moving locally with the advancing fluid is proposed. This introduces complications with respect to keeping track of the relations between the laboratory frame and the frame in which the unmodified GSD equations are valid. Because numerical procedures are used this does not present any practical problem as it would in a purely analytical approach.

Other questions arise as to the validity of the basic GSD concept in such a frame. While the shock discontinuity is inertialess the area–Mach number relations depend on a region around the shock front and thus involve inertial effects which are ignored here. This is felt to be consistent with the general ad-hoc nature of the GSD approach and ultimately must be judged by the experimental evidence. In point of fact the treatment of this problem with no consideration of flow ahead of the shock leads to very similar results. One reason for this is that in the blast-type solution used most of the significant flow effects occur in the period during and right after reflection as the flow amplitude rapidly dies down. To understand the differences introduced by considering the flow field ahead of the shock a plot of the convergence process for the cases $n = 5$ and $n = 6$ with the initial Mach number $M = 2$ is given in figure 9. In figures 9(a) and 9(b) we take account of the flow field ahead created by the outgoing

cylindrical wave. Figures 9(*c*) and 9(*d*) show calculations in which this oncoming flow field is ignored. As discussed above we can see that overall the nature of the convergence process in these cases is similar and results in the formation of polygonal shock fronts periodically changing in orientation. The difference between the cases of taking into account flow ahead of the shock and disregarding it is also clearly seen from this figure. In case of the flow ahead of the shock as in figures 9(*a*) and 9(*b*) the formation of the polygonal shock starts earlier than in the case of no flow ahead. It should be stressed at this point that the later stages of the converging processes are more similar in these two cases. This is due to the fact that the oncoming flow produced by the outgoing cylindrical shock is gradually reduced as the distance from the outgoing shock is increased. This difference becomes even greater when the value of the initial Mach number is increased as discussed earlier in this section.

In conclusion it appears that the proposed mechanism for producing a polygonal reflected shock from a perturbed cylindrical boundary is potentially feasible. In addition we have examined a possibly useful extension of conventional GSD for the treatment of propagation into non-uniform flow regions. It is stressed that this is somewhat ad-hoc and requires experimental investigation in order to asses its proper validity. More ordered approaches to GSD type theories, such as advocated by Prasad (1992), might also be used. The simplicity and extensively examined results of GSD are retained by the present extension. Experiments with devices of the type suggested may be of help in settling this matter.

The authors would like to thank the Swedish Board for Technical Research (TFR) for financial support for this investigation. In addition we would like to thank Göran Gustafsson for discussions and Håkan Gustavsson for help in obtaining support.

REFERENCES

ANDERSON, J. D. 1990 *Modern Compressible Flow*. McGraw-Hill.

APAZIDIS, N. 1992 Control of pressure distribution in shock generators with elliptic cross-sections. *Shock Waves Intl J.* **2**, 147–156.

APAZIDIS, N. 1993 Focusing of weak shock waves on a target in a parabolic chamber. *Shock Waves Intl J.* **3**, 1–10.

APAZIDIS, N. 1994 Focusing of weak shock waves in confined axisymmetric chambers. *Shock Waves Intl J.* **3**, 201–212.

CRAMER, M. S. 1981 The focusing of weak shock waves at an axisymmetric arete. *J. Fluid Mech.* **110**, 249–253.

CRAMER, M. S. & SEEBASS, A. R. 1978 Focussing of weak shock waves at an arête. *J. Fluid Mech.* **88**, 209–222.

DEAR, J. P. & FIELD, J. E. 1987 Applications of the two-dimensional gel technique to erosion problems. *Proc. 7th Intl Conf. on Erosion by Liquid and Solid Impact* (ed. J. E. Field).

DEAR, G. P., FIELD, J. E. & WALTON, A. J. 1988 Gas compression and jet formation in cavities collapsed by shock wave. *Nature* **332**, 505–508.

FRIEDLANDER, F. G. 1958 *Sound Pulses*. Cambridge University Press.

GUSTAFSSON, G. 1987 Focusing of weak shock waves in a slightly elliptical cavity. *J. Sound Vib.* **116**, 137–148.

HAYES, W. D. & PROBSTEIN, R. F. 1966 *Hypersonic Flow Theory*. Academic Press.

HENSHAW, W. D., SMYTH, N. F. & SCHWENDEMAN, D. W. 1986 Numerical shock propagation using geometrical shock dynamics. *J. Fluid Mech.* **171**, 519–545.

LESSER, M. B. & FINNSTRÖM, M. 1987 On the mechanics of a gas-filled collapsing cavity in a liquid. *Proc. 7th Intl Conf. on Erosion by Liquid and Solid Impact* (ed. J. E. Field).

PRASAD, P. 1992 *Propagation of a Curved Shock and Nonlinear Ray Theory*. John Wiley & Sons.

SCHWENDEMAN, D. W & WHITHAM, G. B. 1987 On converging shock waves. *Proc. R. Soc. Lond.* A **413**, 297–311.

SEDOV, L. I. 1946 Propagation of strong blast waves. *Prikl. Mat. Mekh.* **9**, 293–311.

STURTEVANT, B. & KULKARNY, V. A. 1976 The focusing of weak shock waves. *J. Fluid Mech.* **73**, 651–671.

TAYLOR, G. I. 1950 The formation of a blast wave by a very intense explosion. *Proc. R. Soc. Lond.* A **201**, 159–186.

WHITHAM, G. B. 1957 A new approach to problems of shock dynamics. Part 1. Two-dimensional problems. *J. Fluid Mech.* **2**, 145–171.

WHITHAM, G. B. 1959 A new approach to the problems of shock dynamics. Part 2. Three-dimensional problems. *J. Fluid Mech.* **5**, 369–386.

WHITHAM, G. B. 1968 A note on shock dynamics relative to a moving frame. *J. Fluid Mech.* **31**, 449–453.

WHITHAM, G. B. 1974 *Linear and Nonlinear Waves.* John Wiley & Sons.